

k -tilings of the Aztec Diamond

David Keating
University of Wisconsin, Madison

Solvable Lattice Models Seminar
February 22, 2022

Outline

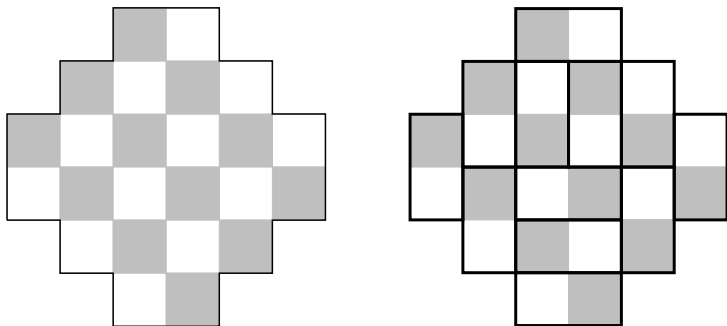
- 1 Review tilings of the Aztec Diamond
 - 1 Relationship with interlacing partitions
 - 2 Relationship with 5-vertex models
- 2 Define a coupling of k 5-vertex models related to the coinversion LLT polynomials
- 3 Construct the coupled k -tilings of the Aztec diamond
- 4 Combinatorial results in certain limits of the coupling parameter

This is joint work with Sylvie Corteel and Andrew Gitlin (arXiv:2202.06020 [math.CO]).

Part 1: The Aztec Diamond

Domino tilings of the Aztec diamond



Domino tilings of the Aztec diamond were first introduced by Elkies, Kuperberg, Larsen, and Propp in 1992.

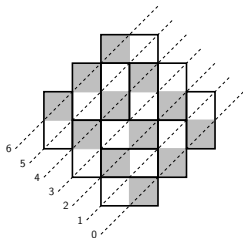


The Aztec diamond of rank $m = 3$ and one possible domino tiling.

Domino tilings of the Aztec diamond

One can add weights to the dominos according to the rules

- A domino of the form  whose top square is on slice $2i - 1$ gets a weight of x_i .
- A domino of the form  whose bottom square is on slice $2i - 1$ gets a weight of y_i .
- All other dominos get a weight of 1.



$$x_1^2 x_2 x_3 y_2^2 y_3^2$$

Domino tilings of the Aztec diamond

Theorem (Elkies, Kuperberg, Larsen, Propp '92)

The partition function of the domino tilings of the rank- m Aztec diamond is given by

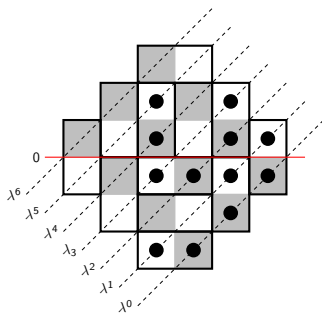
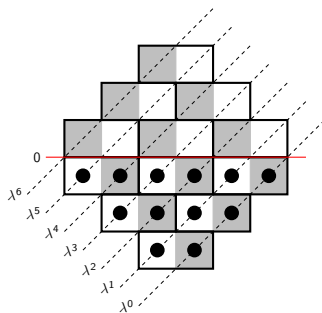
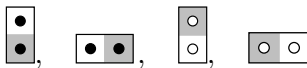
$$Z_{AD}(X_m, Y_m) = \prod_{1 \leq i < j \leq m} (1 + x_i y_j)$$

In particular, if $x_i = y_i = 1$ for $i = 1, \dots, m$, we see that the number of tilings is given by $2^{\binom{m+1}{2}}$.

We'll sketch a vertex model proof of this theorem shortly.

Domino tilings and sequences of partitions

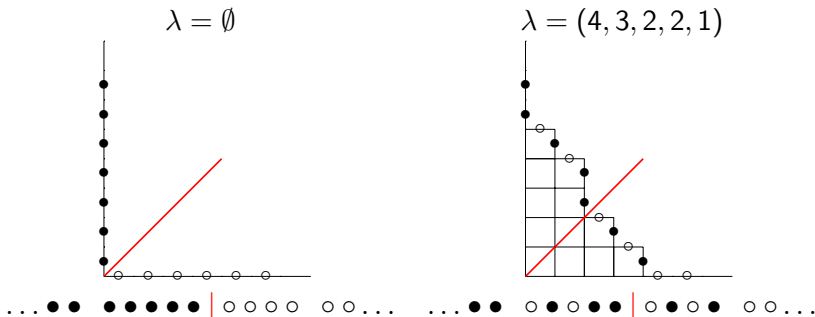
Assign 'particles' and 'holes' to our dominos according to the rules



We think of each diagonal slice as having a string of particles.

Domino tilings and sequences of partitions

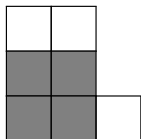
We can identify each string of particles as the Maya diagram of a partition.



In red, we have indicated the 0 content line.

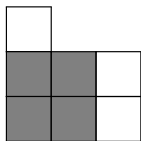
Domino tilings and sequences of partitions

We say that two partitions interlace and write $\mu \preceq \lambda$ if $\lambda_1 \geq \mu_1 \geq \lambda_2 \geq \mu_2 \geq \dots$



$$(2, 2) \preceq (3, 2, 2)$$

We say they co-interlace and write $\mu \preceq' \lambda$ if $\mu' \preceq \lambda'$.



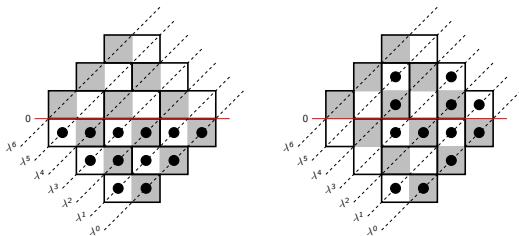
$$(2, 2) \preceq' (3, 3, 1)$$

Domino tilings and sequences of partitions

One can show that specifying a domino tiling is equivalent to specifying a sequence

$$\emptyset = \lambda^0 \preceq' \lambda^1 \succeq \lambda^2 \preceq' \dots \preceq' \lambda^{2m-1} \succeq \lambda^{2m} = \emptyset$$

of interlacing partitions! For example, if every domino is horizontal, then each $\lambda^\ell = \emptyset$, as on the left.

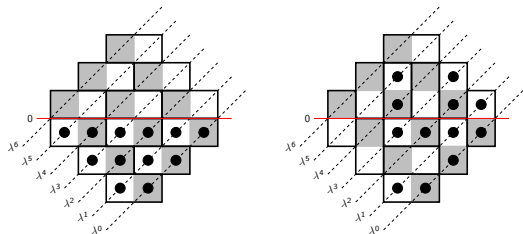


On the right, we have the sequence

$$\emptyset \preceq' (1, 1) \succeq (1, 1) \preceq' (2, 1) \succeq (1) \preceq' (2) \succeq \emptyset$$

Domino tilings and sequences of partitions

With this identification the degree x_i in the weight is given by $|\lambda^{2i-1}| - |\lambda^{2i-2}|$, and for y_i it is given by $|\lambda^{2i-1}| - |\lambda^{2i}|$.



On the left, the tiling has weight 1. On the right, the sequence

$$\emptyset \preceq' (1, 1) \succeq (1, 1) \preceq' (2, 1) \succeq (1) \preceq' (2) \succeq \emptyset$$

has weight

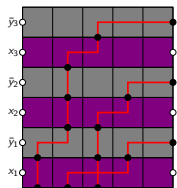
$$x_1^{|(1,1)/(0,0)|} y_1^{|(1,1)/(1,1)|} x_2^{|(2,1)/(1,1)|} y_2^{|(2,1)/(1)|} x_3^{|(2)/(1)|} y_3^{|(2)/(0)|} = x_1^2 x_2 x_3 y_2^2 y_3^2$$

A vertex model formulation

We'll give one more formulation in terms of lattice paths.

- 1 An example of the kind of path configurations we will

consider:

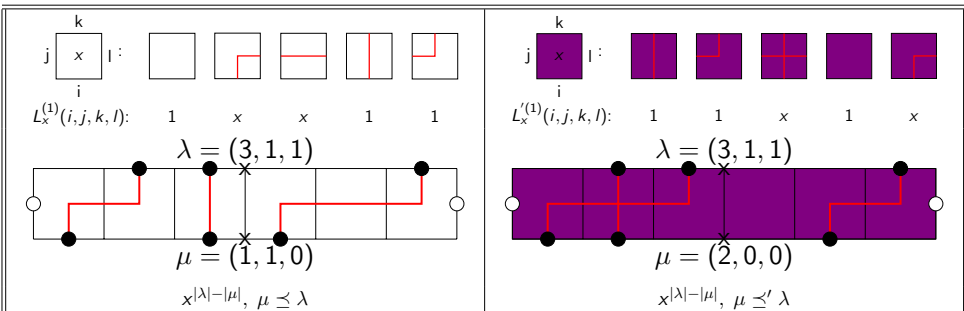


- 2 We will identify the configurations of paths along a horizontal slice with the Maya diagram of a partition.
- 3 The different color faces represent different choices of weights, which will impose different interlacing requirements on these partitions.
- 4 We will choose the weights to match the interlacing conditions we get for the Aztec diamond.

$$\emptyset = \lambda^0 \succ' \lambda^1 \succ \lambda^2 \succ' \dots \succ' \lambda^{2m-1} \succ \lambda^{2m} = \emptyset$$

A vertex model formulation

We consider two different 5-vertex models:



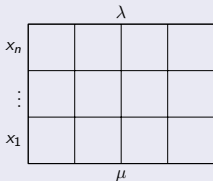
Note: the boundary conditions are given by partitions and they uniquely determine the paths (for a single row).

Aside: Relation to Schur polynomials

Let $s_{\lambda/\mu}(x_1, \dots, x_n) = \sum_{T \in \text{SSYT}(\lambda/\mu)} x^T$ be the skew Schur polynomial.

Proposition

Let $Z_{\lambda/\mu}(x_1, \dots, x_n)$ be the partition function of



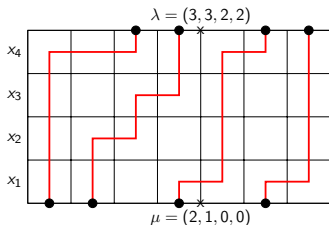
Then $Z_{\lambda/\mu}(x_1, \dots, x_n) = s_{\lambda/\mu}(x_1, \dots, x_n)$.

Aside: Relation to Schur polynomials

For example, consider the following semistandard Young tableaux of shape $\lambda/\mu = (3, 3, 2, 2)/(2, 1)$:

4	4		
2	3		
	1	4	
		1	

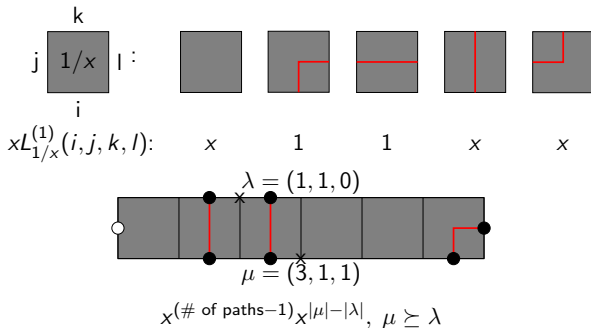
maps to



Both have weight $x_1^2 x_2 x_3 x_4^3$.

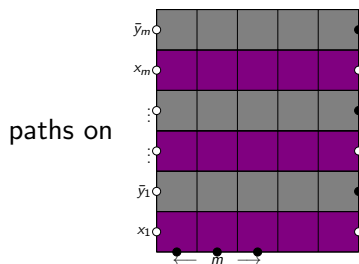
A vertex model formulation

In order to remove cells from a partition we'll need the following change of variables in the white faces:

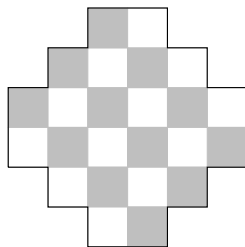


A vertex model formulation

We have a bijection between



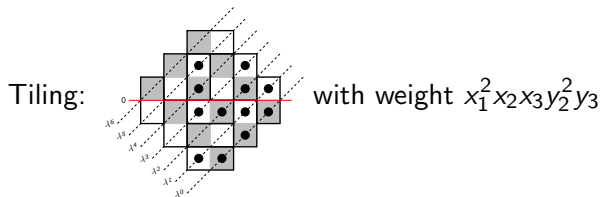
and tilings of



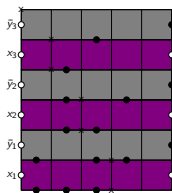
given by looking at the sequence of interlacing partitions.

A vertex model formulation

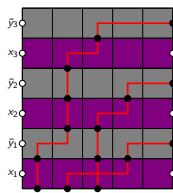
$$\emptyset \preceq' (1, 1) \succeq (1, 1) \preceq' (2, 1) \succeq (1) \preceq' (2) \succeq \emptyset$$



On the other hand, adding the partitions as b.c. to each row



determine the paths



and weight: $(y_1^2 y_2) x_1^2 x_2 x_3 y_2^2 y_3$.

A vertex model formulation

These vertex models satisfy the Yang-Baxter equation (YBE). We have

$$\sum_{\text{interior paths}} w \left(\begin{array}{ccc} & K_3 & \\ J_1 & \begin{array}{c} y \\ 1/x \end{array} & I_3 \\ I_1 & \begin{array}{c} 1/x \\ y \end{array} & J_3 \\ & K_1 & \end{array} \right) = \sum_{\text{interior paths}} w \left(\begin{array}{ccc} & K_3 & \\ J_1 & \begin{array}{c} 1/x \\ y \end{array} & I_3 \\ I_1 & \begin{array}{c} y \\ 1/x \end{array} & J_3 \\ & K_1 & \end{array} \right)$$

for any choice of boundary condition $I_1, J_1, K_1, I_3, J_3, K_3$. Here

$$R_{xy}^{(1)}(i, j, k, l): \begin{array}{c} 1/xj \\ \begin{array}{c} \diagup \diagdown \\ \diagdown \diagup \end{array} \\ y \ i \quad l \end{array} : \begin{array}{ccccc} \begin{array}{c} \diagdown \diagup \\ \diagup \diagdown \end{array} & \begin{array}{c} \diagup \diagdown \\ \diagdown \diagup \end{array} & \begin{array}{c} \diagdown \diagup \\ \diagup \diagdown \end{array} & \begin{array}{c} \diagup \diagdown \\ \diagdown \diagup \end{array} & \begin{array}{c} \diagup \diagdown \\ \diagdown \diagup \end{array} \end{array}$$

$$\begin{array}{ccccc} \frac{1}{1+xy} & \frac{xy}{1+xy} & \frac{1}{1+xy} & \frac{xy}{1+xy} & 1 \end{array}$$

It turns out this makes the partition function of the vertex model simple to compute.

A vertex model formulation

Using the YBE we have

$$\text{Diagram 1} = \text{Diagram 2} = \text{Diagram 3} = \text{Diagram 4} \times (1 + x_1 y_m)^{-1}$$

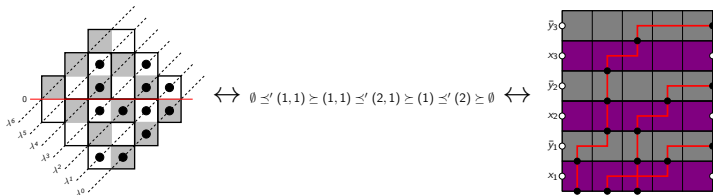
Now repeated applications of the YBE gives

$$\text{Diagram 1} = \text{Diagram 2} \times \prod_{i \leq j} (1 + x_i y_j) = (y_1^{m-1} y_2^{m-2} \dots y_m^0) \prod_{i \leq j} (1 + x_i y_j)$$

It follows that $Z_{AD}(X_m, Y_m) = \prod_{i \leq j} (1 + x_i y_j)$.

Summary so far:

- 1 We showed there is a bijection between tilings of the Aztec diamond and sequences of interlacing partitions.
- 2 We further showed there was a bijection between the sequences of partitions and a certain vertex model.
- 3 In the vertex model formalism we could use the YBE to compute the partition function.



Next...

We repeat this in reverse.

- 1 First, we'll generalize the vertex models.
 - 1 We'll start by defining vertex model realizations of the LLT polynomials.
 - 2 We'll show that this can be thought k coupled 5-vertex models.
 - 3 We'll see that the generalized vertex models still satisfies the YBE.
- 2 From the k coupled 5-vertex models we'll construct the k -tilings.

Part 2: The LLT vertex model

Background

- 1 Lascoux, Leclerc, and Thibon (1997) introduce the LLT polynomials as the generating function of semistandard ribbon tableaux. They count a certain statistic called 'spin.'
- 2 Haglund, Haiman, and Loehr (2005) showed there was an equivalent formulation in terms of tuples of semistandard Young tableaux and a statistic known as 'coinversions'.
- 3 We will use a vertex model formulation of the (supersymmetric) coinversion LLT polynomials describe in Corteel, Gitlin, K., Meza (2020) and Gitlin, K. (2021).
- 4 There is also a vertex model for the (supersymmetric) spin LLT polynomials given by Curran, et al (2021).
- 5 Our vertex weights are degenerations of the vertex model of Aggarwal, Borodin, and Wheeler (2021) coming from the quantum group $U_q(\widehat{\mathfrak{sl}}(2|k))$. In particular, the YBE we will use follows from the YBE of ABW.

The LLT vertex model

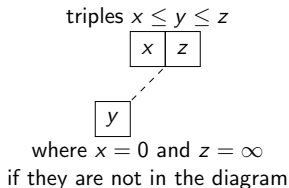
Moral: There is a Yang-Baxter integrable vertex model, related to LLT polynomials, that can be viewed as k interacting copies of the vertex model described previously. These will then map to k interacting domino tilings.

Coinversion LLT polynomials

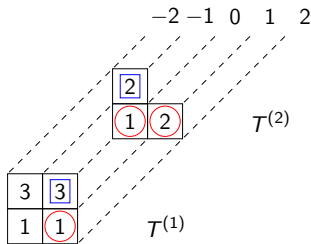
Let $\lambda/\mu = (\lambda^{(1)}/\mu^{(1)}, \dots, \lambda^{(k)}/\mu^{(k)})$ be a tuple of skew partitions.
 Define the coinversion LLT polynomial

$$\mathcal{L}_{\lambda/\mu}(X; t) = \sum_{T \in \text{SSYT}(\lambda/\mu)} t^{\text{coinv}(T)} X^T$$

where **coinversion triples** are given by



For example:

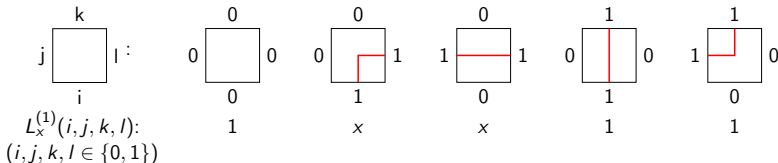


Local weights in the case $k = 1$

If $\lambda/\mu = (\lambda^{(1)}/\mu^{(1)})$ consists of just one skew partition, there can never be any coinversions, so

$$\mathcal{L}_{\lambda/\mu}(X; t) = \sum_{T \in \text{SSYT}(\lambda^{(1)}/\mu^{(1)})} x^T = s_{\lambda^{(1)}/\mu^{(1)}}(X).$$

Therefore, for one color, we can use the weights from the vertex model for Schur polynomials:



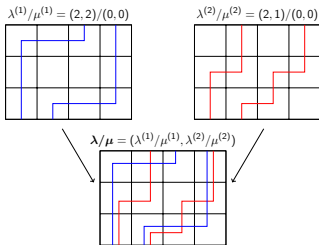
Local weights in the case $t = 1$

Let $\lambda/\mu = (\lambda^{(1)}/\mu^{(1)}, \dots, \lambda^{(k)}/\mu^{(k)})$.

For $t = 1$, the LLT polynomial is a product of Schur polynomials.

$$\mathcal{L}_{\lambda/\mu}(X; 1) = s_{\lambda^{(1)}/\mu^{(1)}}(X) \dots s_{\lambda^{(k)}/\mu^{(k)}}(X)$$

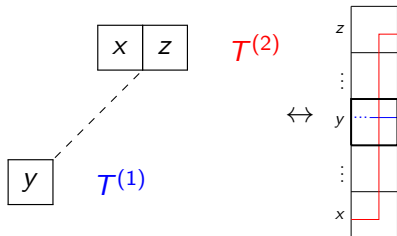
This means we can superimpose the lattice paths:



The weight of the “combined” vertex is the product of the weights from each color.

Local weights in the general case

The coinversion triples can be mapped to a local condition on the vertex model. For instance, when $0 < x < y < z < \infty$,



We get a coinversion if the path of a smaller color exits a face to the right and a path of larger color is present.

Local weights in the general case

Let $i, j, k, l \in \{0, 1\}$. Recall the weights for one color:

$$L_x^{(1)}(i, j, k, l):$$

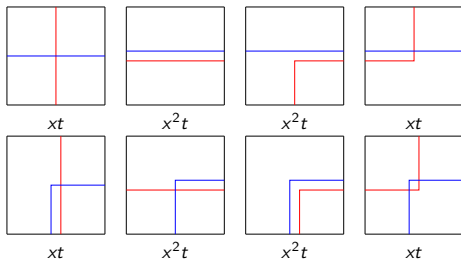
Let $I, J, K, L \in \{0, 1\}^k$, $\mathbf{A} = (A_1, \dots, A_k)$ for $\mathbf{A} \in \{I, J, K, L\}$.
 We introduce t into the weights for k colors

$$L_x^{(k)}(I, J, K, L) = \prod_{i=1}^k L_{xt^{\delta_a}}^{(1)}(I_a, J_a, K_a, L_a)$$

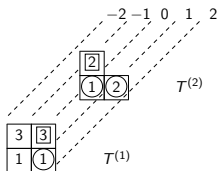
where $\delta_a = \#$ colors greater than a that are present at the vertex.
 In other words, we pick up a factor of t when a color exits right
 and a larger color is present.

An example with 2 colors

With **blue** as color 1 and **red** as color 2, the faces that contribute a factor of t are



As an example:

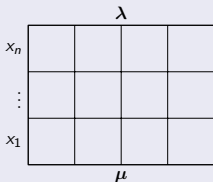


$$W \left(\begin{array}{|c|c|c|c|c|} \hline \text{Blue path} & \text{Red path} & \text{Blue path} & \text{Red path} & \text{Blue path} \\ \hline \text{Red path} & \text{Blue path} & \text{Red path} & \text{Blue path} & \text{Red path} \\ \hline \text{Blue path} & \text{Red path} & \text{Blue path} & \text{Red path} & \text{Blue path} \\ \hline \text{Red path} & \text{Blue path} & \text{Red path} & \text{Blue path} & \text{Red path} \\ \hline \end{array} \right) = x_1^3 x_2^2 x_3^2 t^3$$

The partition function is the coinversion LLT polynomial

Theorem (Corteel, Gitlin, K., and Meza (2020), Aggarwal, Borodin, and Wheeler (2020))

Let λ/μ be a tuple of skew partitions. Let $Z_{\lambda/\mu}$ be the partition function of



Then

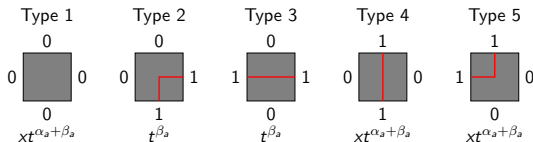
$$Z_{\lambda/\mu}(x_1, \dots, x_n; t) = \mathcal{L}_{\lambda/\mu}(x_1, \dots, x_n; t).$$

The gray weights

We need to generalize the gray faces. We use the substitution

$$J \begin{array}{c} K \\ \square_{\bar{x}} \\ I \end{array} L = x^k t^{\binom{k}{2}} L_{\bar{x}}^{(k)}(I, J, K, L)$$

where $\bar{x} = \frac{1}{xt^{k-1}}$. One can show that the contribution of color i can be given as



where

$\alpha_a = \#$ colors greater than a of Type 1,

$\beta_a = \#$ colors greater than a of Type 4 or 5.

The purple weights

We'll also want to generalize the purple faces. The weights for one color are

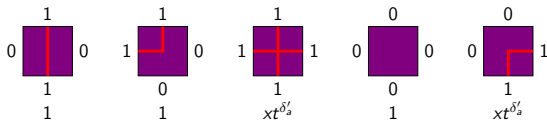
$$L_x^{(1)}(i, j, k, l):$$

and the weights for k colors are

$$L_x^{(k)}(I, J, K, L) = \prod_{i=1}^k L_{xt^{\delta'_a}}^{(1)}(I_i, J_i, K_i, L_i)$$

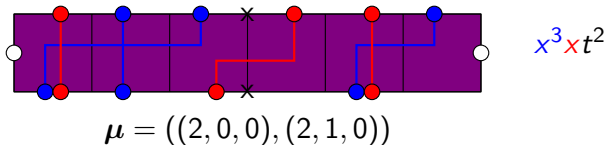
where $\delta'_a = \#$ colors greater than a that are vertical.

The purple weights



$\delta'_a = \#$ colors greater than a that are vertical,

$$\lambda = ((3, 1, 1), (2, 2, 0))$$



$$\mu = ((2, 0, 0), (2, 1, 0))$$

Here **blue** is a smaller color than **red**. In general,

$$x^{|\lambda|-|\mu|} t^{\sum_a \delta'_a}, \mu \preceq' \lambda$$

where $\lambda = \sum_a |\lambda|$ and $\mu \preceq' \lambda$ means $\mu^{(a)} \preceq \lambda^{(a)}$ for each $a = 1, \dots, k$.

With these choices of vertex weight, the YBE still holds.

$$\sum_{\text{interior paths}} w \left(\begin{array}{ccc} & K_3 & \\ J_1 & \begin{array}{c} y \\ \bar{y} \end{array} & I_3 \\ I_1 & \begin{array}{c} \bar{x} \\ y \end{array} & J_3 \\ & K_1 & \end{array} \right) = \sum_{\text{interior paths}} w \left(\begin{array}{ccc} & K_3 & \\ J_1 & \begin{array}{c} \bar{x} \\ y \end{array} & I_3 \\ I_1 & \begin{array}{c} \bar{y} \\ x \end{array} & J_3 \\ & K_1 & \end{array} \right)$$

for any choice of boundary condition $I_1, J_1, K_1, I_3, J_3, K_3$. Here the contribution from color a is given by

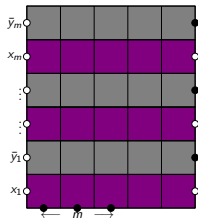
$$\begin{array}{c} \bar{x} \ j \\ \diagdown \ \diagup \\ y \ i \end{array} : \begin{array}{ccccc} \begin{array}{c} \diagup \ \diagdown \\ \diagdown \ \diagup \end{array} & \begin{array}{c} \diagdown \ \diagup \\ \diagup \ \diagdown \end{array} & \begin{array}{c} \diagup \ \diagdown \\ \diagup \ \diagdown \end{array} & \begin{array}{c} \diagdown \ \diagup \\ \diagdown \ \diagup \end{array} & \begin{array}{c} \diagup \ \diagdown \\ \diagup \ \diagdown \end{array} \end{array}$$

$$\frac{1}{1+xyt^{\delta_a}} \quad \frac{xyt^{\delta_a}}{1+xyt^{\delta_a}} \quad \frac{1}{1+xyt^{\delta_a}} \quad \frac{xyt^{\delta_a}}{1+xyt^{\delta_a}} \quad 1$$

where $\delta_a = \#$ colors larger than a that are present. (The total weight at the face is product over all the colors.)

The lattice of interest

A configuration of the lattice



maps to a sequence of interlacing tuples of partitions

$$\mathbf{0} = \lambda^0 \preceq' \lambda^1 \succeq \lambda^2 \preceq' \dots \succeq \lambda^{2m-2} \preceq' \lambda^{2m-1} \succeq \lambda^{2m} = \mathbf{0}$$

where $\mathbf{0} = \underbrace{(\emptyset, \dots, \emptyset)}_k$. In particular, each color satisfies



$$\emptyset = \lambda^0 \preceq' \lambda^1 \succeq \dots \preceq' \lambda^{2m-1} \succeq \lambda^{2m} = \emptyset,$$

that is, it can be mapped to a tiling of the Aztec diamond. We are left to see how the weights map ...

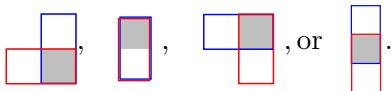
Part 3: k -tilings of the Aztec diamond

Weights of the k -tiling

Consider k tilings $\mathbf{T} = (T_1, \dots, T_k)$ of the Aztec diamond. Assign weights to the dominos according to the rules

- A domino of the form  whose top square is on slice $2i - 1$ gets a weight of x_i .
- A domino of the form  whose bottom square is on slice $2i - 1$ gets a weight of y_i .
- All other dominos get a weight of 1.

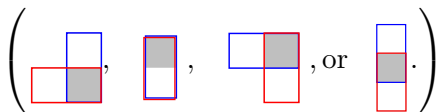
for each color. For every pair of colors $a < b$, each ‘interaction’ gives a power of t where we define ‘interaction’ according to the rule



where here **blue** is a smaller color than **red**.

k -tilings

For example,



$$\lambda^0 = (\emptyset, \emptyset, \emptyset)$$

$$\lambda^1 = ((1, 1), (1, 1, 1), (1))$$

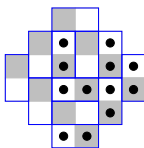
$$\lambda^2 = ((1, 1), (1, 1), \emptyset)$$

$$\lambda^3 = ((2, 1), (1, 1), (1))$$

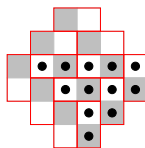
$$\lambda^4 = ((1), (1), \emptyset)$$

$$\lambda^5 = ((2), (1), \emptyset)$$

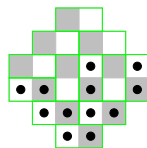
$$\lambda^6 = (\emptyset, \emptyset, \emptyset)$$



T_1



T_2

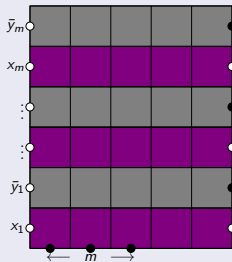


T_3

which has weight $x_1^2 x_2 y_2^2 x_3 y_3^2 x_1^3 y_1 y_2 y_3 x_1 y_1 x_2 y_2 \underbrace{t^4}_{b-r} \underbrace{t^3}_{b-g} \underbrace{t^4}_{r-g}$.

Theorem (Corteel, Gitlin, and K. (2022))

The partition function of the lattice



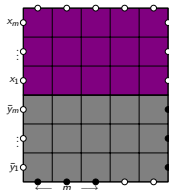
with k colors is equal to $(y_1^{m-1} y_2^{m-2} \dots y_m^{m-m})^k t^{\binom{m}{2} \binom{k}{2}}$ times the partition function of the k -tiling of the Aztec diamond. We have

$$Z_{AD}^{(k)}(X_m; Y_m; t) = \prod_{l=0}^{k-1} \prod_{i \leq j} \left(1 + x_i y_j t^l \right).$$

Proof of the theorem

The proof works just as in the one color case.

- 1 There is a bijection between k -tilings and k -color path configurations going through interlacing sequences of tuples of partitions.
- 2 From the vertex model formulation, the partition function is easy to compute by using the YBE to rearrange the rows of



Some special values of t

$$Z_{AD}^{(k)}(X_m; Y_m; t) = \prod_{\ell=0}^{k-1} \prod_{i \leq j} (1 + x_i y_j t^\ell).$$

Clearly, when $t = 1$ we have

$$Z_{AD}^{(k)}(X_m; Y_m; 1) = (Z_{AD}(X_m, Y_m))^k$$

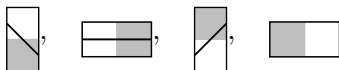
that is, we have k independent tilings of the Aztec diamond. But notice that at $t = 0$ we have

$$\begin{aligned} Z_{AD}^{(k)}(X_m; Y_m; t)|_{t=0} &= \prod_{\ell=0}^{k-1} \prod_{i \leq j} (1 + x_i y_j t^\ell) |_{t=0} \\ &= \prod_{i \leq j} (1 + x_i y_j) = Z_{AD}(X_m, Y_m) \end{aligned}$$

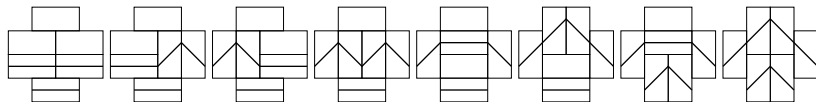
We'd like to give a bijective proof of this. It turns out this is easiest to see in terms of Schröder paths.

$t = 0$ and Schröder paths

For each color, we can assign paths to the dominos according to the following rules:

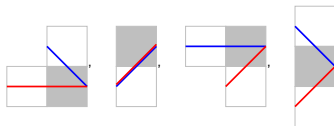


For rank-2 we have



$t = 0$ and Schröder paths


Translating our weights over to the Schröder path picture we have that the power of t is the number of interactions of the form

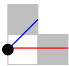
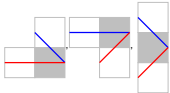


where **blue** is a smaller color than **red**.

$t = 0$ and Schröder paths

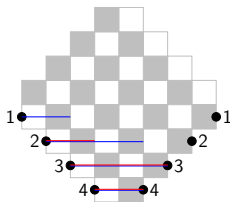
Taking $t = 0$ imposes strict restriction on the Schröder paths.
 Suppose $k = 2$, consider the starting point of the top most paths of each color:

① If  then we get a power of t .

② If  then eventually  and we get a power of t .

③ So when $t = 0$ we are forced to have .

We can repeat this for the other paths. When $m = 4$, the forced paths are



$t = 0$ and Schröder paths

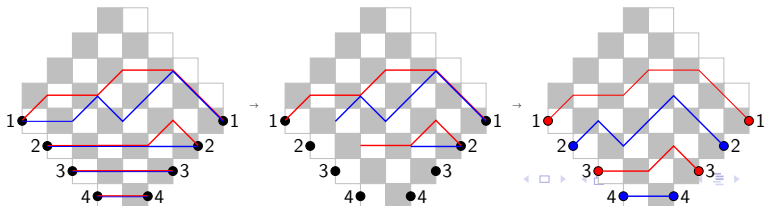
Lemma

The i^{th} path of color 1 is forced to be horizontal for i steps. The i^{th} path of color 2 is forced to be horizontal for $i - 1$ steps.

Proposition

There is a bijection between 2-tilings of the Aztec diamond at $t = 0$ and 1-tilings of the Aztec diamond by removing the frozen paths from the 2-tiling and sliding.

For example,



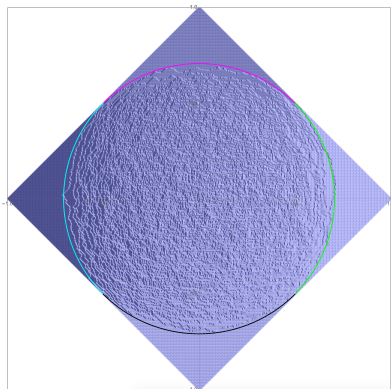
The Arctic circle

It is well-known that tilings of the Aztec diamond exhibit the limit shape phenomenon. As we take the rank to infinity, there are 'frozen' regions in each corner separated from a 'disordered' region in the center by a deterministic curve known as the Arctic curve.

Theorem (Jockusch, Propp,
Schor, '98)

The Arctic curve of the Aztec diamond is given by

$$x^2 + y^2 = \frac{1}{2}.$$



The Arctic circle

Reversing the bijection, allows us to map a single tiling of the Aztec diamond to a *k*-tiling at $t = 0$.

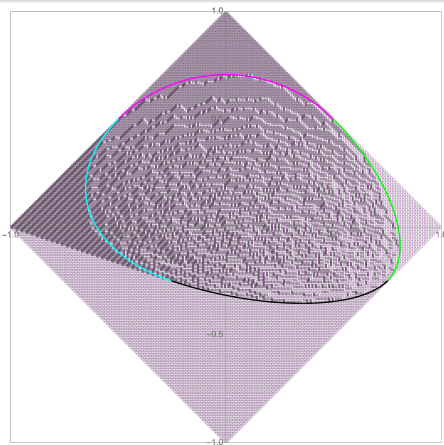
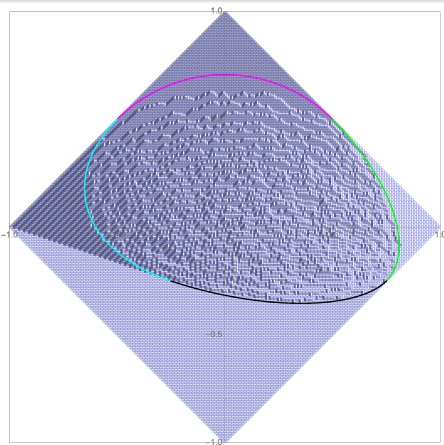
Theorem (Corteel, Gitlin, K.)

The arctic curve for 2-tilings of the Aztec diamond when $t = 0$ is given by

$$\left\{ \begin{array}{ll} x^2 + y^2 = \frac{1}{2}, & x \in [-1/2, 1/2], y > 1/2 \\ (x + y)^2 + (2y)^2 = \frac{1}{2}, & x \in [-1/4, 3/4], y < -1/4 \\ \left(\frac{3x+y-1}{2}\right)^2 + \left(\frac{3y+x-1}{2}\right)^2 = \frac{1}{2}, & y \in [-1/4, 1/2], x > -\frac{1}{3}y + \frac{2}{3} \\ \left(\frac{3x+y-1}{4}\right)^2 + \left(\frac{5y-x-1}{4}\right)^2 = \frac{1}{2}, & y \in [-1/4, 1/2], x < -\frac{1}{3}y - \frac{1}{3} \end{array} \right.$$

for both colors.

The Arctic circle



Simulation of a 2-tiling of the rank-128 Aztec diamond at $t = 0$ with the computed Arctic curve overlaid.

$t \rightarrow \infty$

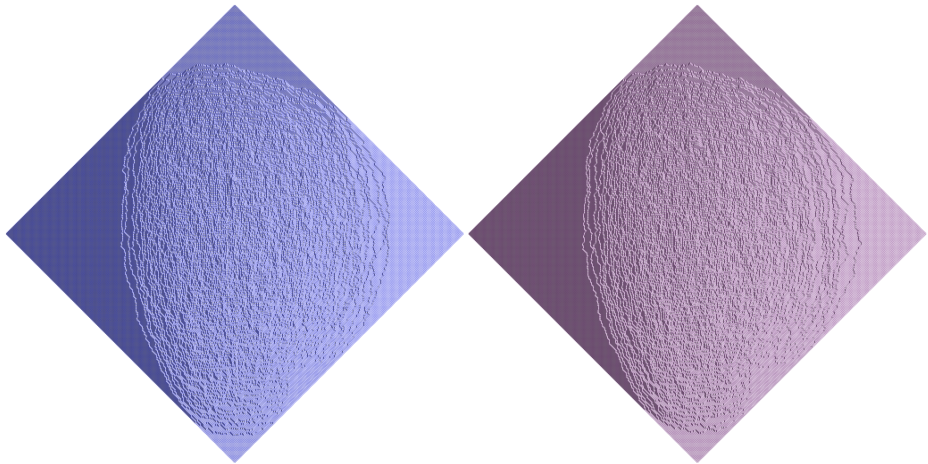
Lemma (Corteel, Gitlin, K.)

Let \mathbf{T} be a k -tiling of the Aztec diamond of rank m with j interactions. Let $\phi(\mathbf{T})$ be the involution that flips the tilings across the line $y = x$. Then $\phi(\mathbf{T})$ is a k -tiling of the Aztec diamond of rank m with $\binom{k}{2} \binom{m+1}{2} - j$ interactions.

Proposition (Corteel, Gitlin, K.)

There is a bijection between tilings of the Aztec diamond at $t = 0$ and tilings of the Aztec diamond in the limit $t \rightarrow \infty$ given by reflecting across the line $y = x$. In particular, the Arctic curve in the limit $t \rightarrow \infty$ is the same as that for $t = 0$ up to the reflection.

Other values of t ?



Simulation of a 2-tiling of the rank-256 Aztec diamond at $t = 5$.

Summary

- 1 We can use the machinery from the LLT vertex model to construct a model of k coupled tilings of the Aztec diamond and compute its partition function.
- 2 In certain limits of the coupling parameter ($t = 0, 1, \infty$) we have bijections relating the k -tilings to the usual 1-tilings.
- 3 We know that the model has a symmetry with respect to mapping $t \mapsto \frac{1}{t}$.
- 4 It would be interesting to study if there are k -tiling generalizations of, say, the domino shuffle algorithm.
- 5 It would very interesting to understand the asymptotic behavior for values t outside of the special cases.

End!

- [1] A. Aggarwal, A. Borodin, and M. Wheeler. "Colored Fermionic Vertex Models and Symmetric Functions." *Preprint arXiv:2101.01605*, 2021.
- [2] S. Corteel, A. Gitlin, D. Keating, and J. Meza. "A vertex model for LLT polynomials." *Preprint arXiv:2012.02376*, 2020.
- [3] S. Corteel, A. Gitlin, and D. Keating. "Colored vertex models and k -tilings of the Aztec diamond." *Preprint arXiv:2202.06020*, 2022.
- [4] M. Curran, C. Frechette, C. Yost-Wolff, S. Zhang, and V. Zhang. "A lattice model for Super LLT polynomials." *Preprint arXiv:2110.07597*, 2021.
- [5] N. Elkies, G. Kuperberg, M. Larsen, and J. Propp. "Alternating-sign matrices and domino tilings. I." *J. Algebraic Combin.*, 1(2):111-132, 1992.
- [6] N. Elkies, G. Kuperberg, M. Larsen, and J. Propp. "Alternating-sign matrices and domino tilings. II." *J. Algebraic Combin.*, 1(3):219-234, 1992.
- [7] A. Gitlin and D. Keating. "A vertex model for supersymmetric LLT polynomials." *Preprint arXiv:2110.10273*, 2021.
- [8] J. Haglund, M. Haiman, and N. Loehr. "A combinatorial formula for Macdonald polynomials." *Journal of the American Mathematical Society*, 18(3):735-761, 2005.
- [9] W. Jockusch, J. Propp, and P. Shor. "Random domino tilings and the arctic circle theorem." *Preprint arXiv:9801068*, 1998
- [10] A. Lascoux, B. Leclerc, and J.-Y. Thibon. "Ribbon tableaux, Hall-Littlewood functions, quantum affine algebras, and unipotent varieties." *Journal of Mathematical Physics*, 38(2):1041-1068, 1997.

Thank You!